Annals of Biomedical Engineering, Vol. 26, pp. 608–617, 1998
Printed in the USA. All rights reserved.

Mathematical Modeling of the First Inflation of Degassed Lungs

BÉLA SUKI,* JOSÉ S. ANDRADE, JR.,† MARK F. COUGHLIN,* DIMITRIJE STAMENOVIĆ,*
H. EUGENE STANLEY,‡ MAMATHA SUJEER,* AND STEFANO ZAPPERI‡

*Department of Biomedical Engineering, Boston University, Boston, MA, †Departamento de Física, Universidade Federal do Ceará, 60451-970 Fortaleza, Ceará, Brazil, and ‡Center for Polymer Studies, Department of Physics, Boston University, Boston, MA

(Received 10 June 1997; accepted 30 November 1997)

Abstract—The pressure–volume ($P-V$) relationship of degassed lungs during the first inflation is different from that in consecutive inflations. We developed a mathematical model of the $P-V$ curve of the first inflation by assuming that (1) central airways are open leading to many subtrees of n generations that are initially closed; (2) an airway opens when inflation pressure reaches the opening threshold pressure of that segment; and (3) the opening threshold pressures do not depend on airway generation. In this model, airway opening occurs in cascades or avalanches. To test the model which contains only two parameters, n and a pressure, P_{low}, at which at least one subtree completely opens, we measured the first inflation $P-V$ curves of 15 excised and degassed rabbit lungs. By fitting these data, we found that $n=17\pm5$, $P_{low}=23\pm4$ cmH_2O, and that there is a wide distribution of threshold pressures for airways with diameters <2 mm. Analysis of the $P-V$ curve in a lung which was lavaged with a liquid of constant surface tension and in which airways are presumably open demonstrated that the distribution of threshold pressures is narrow, and hence no avalanches occur during inflation. We conclude that in normal lungs the first inflation is dominated by avalanche behavior of airway opening providing information on the global distribution of threshold pressures and the average site of airway closure. © *1998 Biomedical Engineering Society.*
[S0090-6964(98)00404-4]

Keywords—Pressure-volume curve, Airways, Alveoli, Avalanches, Surface tension.

INTRODUCTION

The pressure-volume ($P-V$) relationship of mammalian lungs have been the object of numerous studies for more than half a century.[1,3,5,10,12,17,20,22,26,27] Before any $P-V$ measurements are carried out in excised lungs, the standard procedure is to first degas the lungs in a vacuum chamber. Following this procedure, the $P-V$ loops are collected under various conditions. It is well established that the very first inflation $P-V$ curve of the lung from its degassed state is completely different from all consecutive inflation curves. Unfortunately, very few first inflation curves have been published. Frazer and Weber[5] studied the $P-V$ curves of excised rat lungs. They showed that starting from the degassed state, transpulmonary pressure (P_{tp}) first increases rapidly without noticeable change in V followed by a sudden transition to a state where P_{tp} is almost constant but V increases steeply. This transition is in some cases so sharp that the $P-V$ curve is similar to a step change in V. These data also revealed that P_{tp} can even decrease during inflation, provided the inflation flow rate is high. To our knowledge, no quantitative description has been offered as to why the first inflation is so different from all consecutive ones. The goal of this study is to provide a quantitative analysis of the $P-V$ relationship during the first inflation.

We hypothesized that airway reopening dominates the first inflation, whereas consecutive inflations are less influenced by airway reopening and are governed primarily by the mechanical properties of the alveolar surface film and the connective tissue of the parenchyma. We tested this hypothesis by deriving a mathematical model of the alveolar volume distribution during inflation based on the concept that airways open collectively in bursts or avalanches.[2,25] We then used this model to analyze the initial $P-V$ curves starting from the degassed state of excised rabbit lungs.

THEORY

We first briefly describe the mechanism of airway opening which is based on the ensemble behavior of airway openings in a tree structure.[2,25] Next, we derive the $P-V$ relationship for the case of lung inflation from the degassed state.

We simulated lung inflation by applying a transpulmonary pressure P_{tp} across the airway tree and gradually increasing P_{tp} at a uniform rate. Experiments on flexible tube models[6] as well as in airways[11] suggest that in order

Address correspondence to Béla Suki, Ph.D., Dept. of Biomedical Engineering, Boston University, 44 Cummington St., Boston, MA 02215. Electronic mail: bs@enga.bu.edu

to open an airway segment a critical threshold pressure must be overcome. When the pressure difference across the airway segment reaches this critical value, the airway opens in a fraction of a second which is negligible compared to inflation time. Thus, we assign an opening threshold pressure (p_{th}) to each closed airway segment and consider the opening process of one airway to be instantaneous. The opening of one airway is a dynamic and local process.[6,27] Airways do not open individually, but in a sequence of avalanches.[25] Thus, the dynamics of airway opening in a tree cannot be handled as an isolated phenomenon. The essence of this process is as follows. When P_{tp} exceeds the p_{th} of an airway segment, that airway opens almost instantaneously. However, one or both daughter airways that had a p_{th} smaller than P_{tp} (or had been opened) will also open almost simultaneously with the parent (or be connected to the top of the tree). This process of sequentially opening airways continues to propagate until no more airways can be opened by the current value of P_{tp}. The number of airways opened depends on the size of the subtree and the distribution of p_{th} in the subtree and can thus vary considerably. Such a process of bursts, triggered by overcoming a threshold, is called an avalanche. The avalanche theory was based on measured resistance of the terminal airways during inflation which was found to decrease in discrete steps.[14–16] The above avalanche model of airway openings predicts that the distribution of the discrete jumps in the terminal airway resistance is a power law in agreement with that derived from experimental data.[25]

Before applying the above ideas to the $P-V$ relationship along the first inflation curve, we first introduce two normalized pressures: P is the ratio of P_{tp} to the maximum P_{tp} ($P_{tp,max}$) at total lung capacity (TLC) representing the normalized external pressure, and p is the normalized opening threshold pressure, i.e., $p=p_{th}/P_{tp,max}$. Thus, both normalized pressures take values between 0 and 1. We model the airways as a binary branching tree with N generations. We assume that at the beginning of inflation, the first $N-n$ generations constituting the central airways, are open and all airways in the last n generations are closed.

The branching system in the central airways is not necessarily symmetric; what is required is that the number of subtrees (L) so defined is large (note that $L=2^{N-n}$ if the central part is symmetric). However, the branching within a subtree is taken to be symmetric, that is the number of alveoli attached to the terminal ends in each subtree is 2^n. We further assume that subtree i($i=1,...,L$) has a maximum prssure, $P_{max,i}$, at which the subtree completely opens. In other words, the opening threshold pressures p_i in subtree i are random variables distributed in the interval from 0 to $P_{max,i}$ according to a probability density distribution $f(p)$; that is the shape of $f(p)$ is independent of i. Additionally, the $P_{max,i}$ values are also random variables and are distributed uniformly in the interval from P_{low} to 1. Thus P_{low} represents the lowest pressure at which at least one subtree will become completely opened.

The volume contained in the airways is less than 10% of the total lung volume. Hence we take lung volume to be proportional to the number of alveoli, σ, that are open at a given P. We define an alveolus open if it is not collapsed and there is a continuous pathway along which all airway segments are open so that the alveolus is connected to the trachea. If n is large, σ can be sufficiently approximated by its average value, which can be calculated using the hierarchial structure of the tree.[29]

We first examine the $P-V$ relations corresponding to airway openings via avalanches in one subtree. If the external pressure in the accessible region is P, then the probability that an airway is open is equal to the area under the probability density distribution $f(p)$ from 0 to P which is just the cumulative distribution function of the thresholds pressures, $F(P)$. In a given subtree i, if P is less than $P_{max,i}$ then the probability that an airway is open is $\alpha=F(P,P_{max,i})$ where we explicitly noted the dependence of F on $P_{max,i}$. The reason is that in subtree i, the opening threshold pressures are distributed between 0 and $P_{max,i}$ and hence we require that $F(P_{max,i},P_{max,i})=1$. Let us assume now that in a k-generation subtree the average number of open airways is $\overline{\sigma_k}$. Then, according to Fig. 1, the average number of open airways at generation $k+1$, $\overline{\sigma_{k+1}}$, can be related to $\overline{\sigma_k}$ as follows. There are three different possibilities for $\overline{\sigma_{k+1}}$: (A) When both k-generation subtrees are connected, we obtain $\overline{\sigma_{k+1}}=2\overline{\sigma_k}$ with probability α^2 since the probability that an airway segment is open is α. (B) and (C) Only one subtree is connected and $\overline{\sigma_{k+1}}=\overline{\sigma_k}$ with probability $2\alpha(1-\alpha)$. (D) No subtrees are connected so that $\overline{\sigma_{k+1}}=0$ with probability $(1-\alpha)^2$. Thus, we can set up the following recursion relationship:

$$\overline{\sigma_{k+1}}=\alpha^2 2\overline{\sigma_k}+2\alpha(1-\alpha)\overline{\sigma_k}+(1-\alpha)^2 0=2\alpha\overline{\sigma_k}. \tag{1}$$

This recursion relationship can be solved for an n-generation tree yielding the number of open alveoli as

$$\overline{\sigma(P,P_{max,i})}\equiv\overline{\sigma_k}=\begin{cases}2^n F(P,P_{max,i})^n, & 0<P\leq P_{max,i},\\ 2^n, & P_{max,i}<P\leq 1,\end{cases} \tag{2}$$

where we have substituted α with $F(P,P_{max,i})$ as well as included the case $P>P_{max,i}$ which corresponds to a completely open subtree.

The total volume or the total number of open alveoli is obtained by summing Eq. (2) over all subtrees

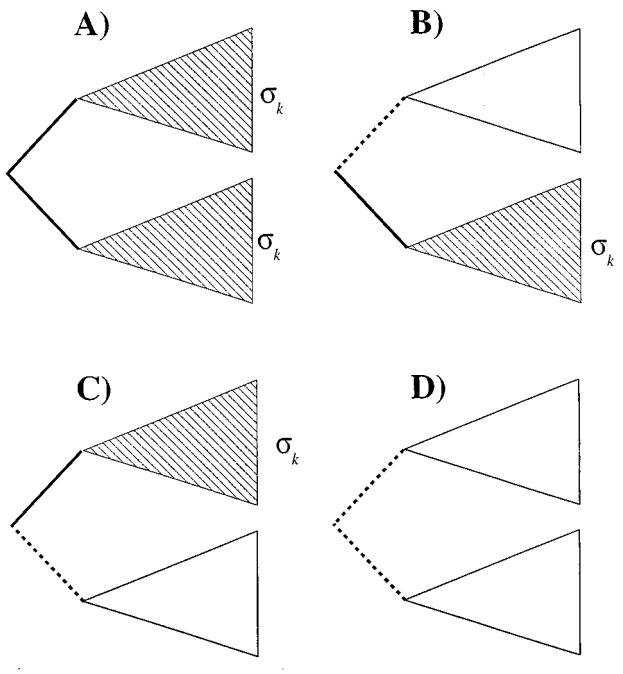

FIGURE 1. Schematic diagram of the avalanches in a tree. Shaded and empty triangles denote subtrees of size σ_k that are connected and not accessible, respectively. Thick and dashed lines are open and closed airways, respectively. (A) Both subtrees become connected at generation $k+1$; (B) and (C) only one subtree is connected; and (D) none of the subtrees are connected. See the text for further explanations.

$$\sigma_{\mathrm{tot}}(P)=\sum_{i=1}^{2^{N-n}}\overline{\sigma(P,P_{\mathrm{max},i})}\cong 2^{N-n}\langle\overline{\sigma(P)}\rangle, \qquad (3)$$

where the angular brackets denotes averaging over all values of $P_{\mathrm{max},i}$ as follows:

$$\langle\overline{\sigma(P)}\rangle=\frac{1}{1-P_{\mathrm{low}}}\int_{P_{\mathrm{low}}}^{1}\overline{\sigma(P,P_{\mathrm{max},i})}\,dP_{\mathrm{max}}. \qquad (4)$$

Equation (4) cannot be solved for the general case, i.e., an arbitrary distribution of thresholds. We therefore examine two special cases which yielded two different model types.

Model 1

In this model, we assume that the probability density distribution $f(p)$ is uniform and therefore the cumulative distribution of the thresholds is

$$F(P,P_{\mathrm{max},i})=\begin{cases}P/P_{\mathrm{max},i}, & 0<P\leqslant P_{\mathrm{max},i},\\ 1, & P_{\mathrm{max},i}<P\leqslant 1.\end{cases} \qquad (5)$$

To solve Eq. (4) using Eq. (5), we consider the two cases, $P<P_{\mathrm{low}}$ and $P>P_{\mathrm{low}}$, separately. For $P<P_{\mathrm{low}}$, we obtain

$$\langle\overline{\sigma(P)}\rangle=\frac{(P_{\mathrm{low}}^{1-n}-1)2^n}{(1-P_{\mathrm{low}})(n-1)}\,P^n. \qquad (6)$$

For $P>P_{\mathrm{low}}$, we split the integral in Eq. (4) into two parts:

$$\langle\overline{\sigma(P)}\rangle=\frac{1}{1-P_{\mathrm{low}}}\left(\int_{P_{\mathrm{low}}}^{P}\overline{\sigma(P,P_{\mathrm{max},i})}\,dP_{\mathrm{max}}+\int_{P}^{1}\overline{\sigma(P,P_{\mathrm{max},i})}\,dP_{\mathrm{max}}\right),$$

and the two integrals can be easily evaluated using Eq. (2)

$$\langle\overline{\sigma(P)}\rangle=\frac{2^n}{1-P_{\mathrm{low}}}\left[(P-P_{\mathrm{low}})+\frac{P-P^n}{1-n}\right]. \qquad (7)$$

Equations (6) and (7) can be used to describe the complete $P-V$ relationship of the model as follows. For $P<P_{\mathrm{low}}$, the volume or the average number of communicating alveoli in a subtree is proportional to P^n. When $P\approx 1>P_{\mathrm{low}}$, the volume is dominated by the first term in Eq. (7). The transition at $P=P_{\mathrm{low}}$ is also smooth, and Eqs. (6) and (7) as well as their derivatives with respect to P are equal.

Finally, when $P=1$, Eq. (7) gives 2^n, that is the number of alveoli in one n-generational subtree. Thus, we divide Eqs. (6) and (7) with 2^n, to obtain the $P-V$ relationship where both volume V and pressure P are normalized with their respective values at TLC:

$$V(P)=\begin{cases}\dfrac{P_{\mathrm{low}}^{1-n}-1}{(1-P_{\mathrm{low}})(n-1)}\,P^n, & P\leqslant P_{\mathrm{low}},\\ \dfrac{1}{1-P_{\mathrm{low}}}\left(P-P_{\mathrm{low}}+\dfrac{P^n-P}{n-1}\right), & P_{\mathrm{low}}<P\leqslant 1.\end{cases} \qquad (8)$$

Equation (8) constitutes our final model which is now suitable to be compared with experimental data. There are only two parameters in the model. The first is P_{low} which represents the lowest pressures at which one subtree becomes fully open. The second parameter is n, the order of the subtree in which we assumed that all airways are closed at the beginning of inflation and which opens via avalanches. The value of P_{low} primarily determines where the step-like transition in volume oc-

curs whereas n provides the sharpness of the increase in volume.

Model 2

We now assume that the subtrees have identical threshold pressure distribution, i.e., $P_{\max,i}=1$ $(i=1,...,N-n)$ and hence $F(P,P_{\max,i})=F(P)$. In this case, we can also retain the general form of the cumulative distribution of the threshold pressures, and the normalized $P-V$ curve is quite simple:

$$V(P)=F(P)^n. \tag{9}$$

In this $P-V$ model, the parameters are the order of the tree, n, and any parameters necessary to specify $F(P)$. For simplicity, we only examine one special distribution: $f(p)$ is uniform between two values, a and b (where $0 \leqslant a \leqslant b \leqslant 1$) and zero outside. The corresponding $P-V$ model is

$$V(P)=\left[\frac{P-a}{b-a}\right]^n. \tag{10}$$

Note that depending on the two parameters a and b, the distribution may give rise to a threshold pressure distribution which is either wide or quite narrow with a sharp peak. The special case when $a=0$ and $b=1$, the $P-V$ model takes a particularly simple form with a single parameter n, the order of the tree where closure occurs:

$$V(P)=P^n. \tag{11}$$

METHODS

Lung Preparation

New Zealand White rabbits of either sex and body weight between 1.8 and 3.0 kg were sacrificed by an overdose of pentobarbital sodium. The chest wall was opened and the lung, trachea and heart were excised *en bloc*. After removal of excess tissues (e.g., heart, esophagus, fat), a cannula was inserted into the trachea and the lung was degassed in a vacuum chamber according to Smith and Stamenović[20] after which they were slowly brought back to atmospheric pressure.

Experimental Setup

Lung volume V was controlled with an apparatus for continuous inflation–deflation of excised lungs described previously.[21] Briefly, the device consisted of two communicating concentric cylinders. Both cylinders were half-filled with water. The water in the inside cylinder moved air into the lung. The volume of the displaced water was considered to be the volume of air entering the lung. The change in water height in the inside cylinder was measured by a pressure transducer and calibrated as the air volume. Transpulmonary pressure P_{tp} was measured in the tracheal outlet. Validyne model MP45-28-871 (± 50 cmH_2O) pressure transducers and Validyne CD19A carrier demodulators were used to monitor pressure–volume $P-V$ data. Both pressure and volume signals during the first and second inflation and deflation cycles were sampled at 53 Hz by Data Translations DT2811 DAS and analog-to-digital converter. Data were stored by ALS 80486/25 MHz computer for off-line analysis.

Protocol

The degassed lungs were suspended from the tracheal cannula, attached to the apparatus for the $P-V$ measurements. The lungs were inflated to 30 cmH_2O, then deflated to zero P_{tp} and reinflated to 30 cmH_2O. A single cycle took ~90 s. Lungs trapping excess air were discarded. All measurements were performed at the room temperature of 27 °C. During measurements the lungs were kept moist by frequent spraying with a physiological saline solution. Measurements were made in 15 lungs.

Data Analysis and Modeling

To obtain normalized $P-V$ curves, the measured pressure and volume data were first scaled by the corresponding pressures and volumes at TLC. There was a small constant positive component of the volume signal (corresponding to tissue volume) which was numerically removed from the data. The normalized $P-V$ curves were then fit by the models given by Eqs. (8) and (10) using a global optimization algorithm[4] which minimized the root-mean-square error between measured and model simulated volume. The model parameters are given as mean $\pm$ one standard deviation and compared using paired t tests.

RESULTS

Two typical examples of the $P-V$ curves measured in two excised rabbit lungs are shown in Fig. 2. Note that in both cases the first inflation is qualitatively different from the second inflation. The first inflation $P-V$ curve in Fig. 2(A) shows a steep increase in volume similar to a power-law function. The first $P-V$ curve in Fig. 2(B) also shows a sharp increase in V. However, the pressure then temporarily decreases and then increases again. Seven out of the 15 lungs we studied displayed the behavior shown in Fig. 2(B). Since the models given by Eqs. (8) and (10) are not consistent with this behavior, we only analyzed the $P-V$ curves of the eight lungs which were similar to that in Fig. 2(A).

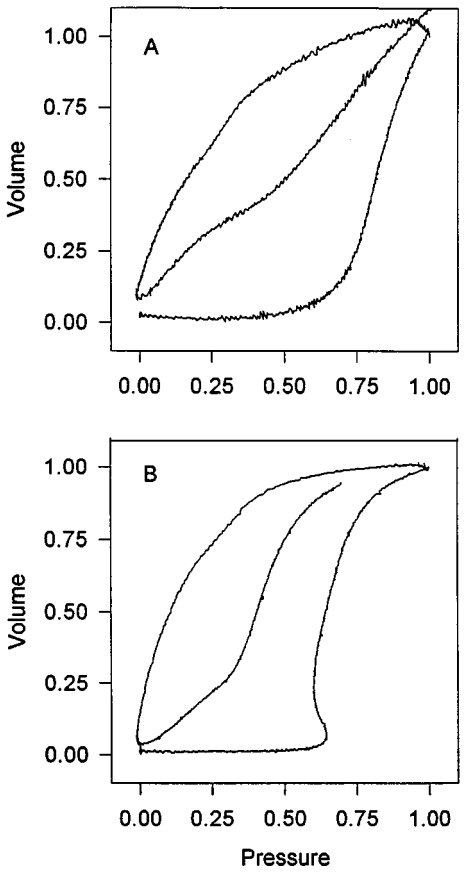

FIGURE 2. Two representative examples of the normalized pressure–volume curves. Inflation starts from the degassed state at zero volume and negative pressure. Note that the second inflation is very different from the first one. (A) *P–V* curve of lung No. 16 where the volume is a power-law function of pressure; (B) *P–V* curve of lung No. 29 where pressure displays a decrease after the initiation of volume increase.

Figure 2(A) also shows that following the sharp increase in volume, the rate of change of this volume increase starts decreasing at high pressures (>0.8). Model 2 being a simple power law [Eq. (10)] is not consistent with this behavior whereas model 1 [Eq. (8)] may give rise to this phenomenon. To be able to compare the performances of the two models, we only fit the data in the region where the rate of change in volume increase did not decrease ($P<0.85$).

The models provided very good fits to these data as exemplified in Fig. 3. The weights and TLCs of the lungs, the inflation flow rates, the errors, and the optimal parameters corresponding to both models are given in Table 1. Except for lungs 15 and 21, model 1 tended to provide smaller errors despite the fact that it has one less parameter than model 2. The difference between the errors was not statistically significant. The error did not correlate significantly with weight, TLC, or inflation rate.

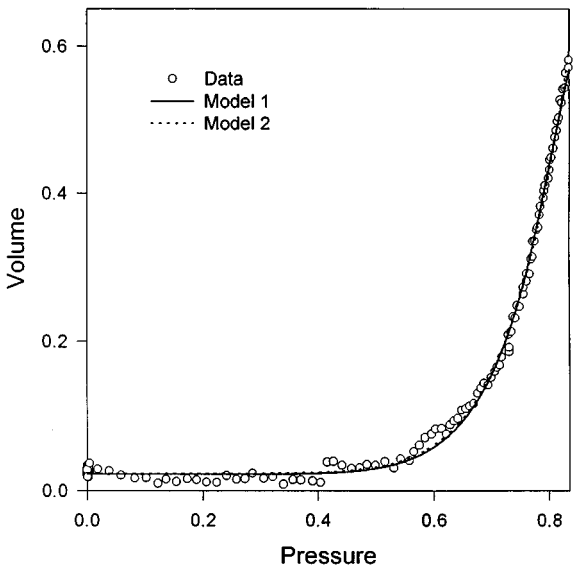

FIGURE 3. Normalized pressure–volume curve of lung No. 16 (symbols) and the fit of model 1 defined by Eq. (8) (solid line) and model 2 defined by Eq. (10) (dashed line).

The average order of the subtrees in which the model assumed a complete closure at the beginning of the first inflation was 17 ± 5 in both models (their difference was not statistically significant). In model 1, the relative pressure threshold at which one subtree completely opens was 0.79 ± 0.12 which corresponds to P_{tp} of 23.4 ± 3.6 cmH_2O. The parameter b in model 2 correlated strongly with P_{low} (correlation coefficient 0.97); however, b was statistically significantly higher than P_{low}. Interestingly, parameter a was very close to zero. There was no correlation between the weight, TLC, or inflation rate and n. However, there was a negative correlation between P_{low} and TLC (correlation coefficient 0.91) and a weaker correlation between P_{low} and inflation rate (correlation coefficient 0.64).

DISCUSSION

In this study we have developed two mathematical models of airway opening based on statistical mechanical principles and applied them to the first inflation of excised lungs from their degassed state. The basis of the model is the statistical process of recruitment of alveoli via an avalanche-like airway opening. Indeed, the recruitment of lung units has recently been shown to account for much of lung hysteresis.[3] The significance of the present modeling effort is that we quantified the recruitment process which, based on global $P-V$ measurements made at the airway opening, allowed us to predict the site of airway closure. It is noteworthy that this information was independent of whether we ana-

TABLE 1. Weight of lungs, flow rates, and the parameters obtained from model fitting. W, weight of lobe; TLC, total lung capacity; Flow, volumetric inflation rate; n, order of tree in the models; P_{low}, a, and b are pressures defining the distribution of thresholds (see the text). Error is 10^{-3} times the root-mean-square error between data and models.

				Model 1			Model 2			
Lung #	W (g)	TLC (ml)	Flow (ml/s)	n	P_{low}	Error	n	a	b	Error
9	8.4	82	7.1	18.8	0.87	6.6	17.8	0	0.93	16.9
14	8.8	73	8.3	17.5	0.96	7.0	17.7	0	0.97	7.5
15	11.7	77	12.6	15.1	0.97	14.3	20.4	0	0.95	11.0
16	9.9	81	13.3	8.3	0.81	7.2	8.3	0	0.89	7.2
21	7.6	95	17.9	25.4	0.54	29.4	24.9	0	0.61	8.7
23	10.5	98	12.8	18.7	0.66	3.5	13.5	0	0.79	3.9
27	14.0	97	12.6	16.0	0.61	5.3	18.5	0	0.69	6.5
32	9.4	86	13.4	16.0	0.89	3.6	16.2	0	0.93	3.2
Mean	10.0	86	12.3	17.0	0.79	9.6	17.2	0	0.85	8.1
SD	2.0	10	3.3	4.8	0.16	8.7	4.9	0	0.13	4.3

lyzed the $P-V$ data with model 1 or model 2. This indicates that the avalanche mechanism does capture the essence of the data and hence with regard to the global $P-V$ relationship, the collective behavior of airway opening may be more important than the manner in which individual airways reopen. Before discussing the physiological implications of our results we first evaluate the relevance of the models with regard to several mechanisms that have been simplified or neglected from the analysis.

Model Assumptions

The essence of the models is that they incorporate the ensemble behavior of the airway opening in a tree structure: airways do not open individually, the opening of one airway can initiate the opening of subtended airways leading to a cascade or avalanche of airway openings.[2,25] Using this avalanche mechanism, we calculated the average number of alveoli that open as a function of pressure. Since we used a symmetric binary tree in the calculations, we derived closed-form solutions which allowed us to analyze experimentally obtained $P-V$ curves. Although the airway tree is asymmetric, we do not expect that the symmetry assumption introduces serious limitation in our case since the last 5–10 generations of the bronchial tree are not grossly asymmetric.[8] Indeed, using numerical simulations, we have recently shown that the distribution of recruited alveolar volumes and hence the $P-V$ curve does not depend on asymmetry.[24] Additionally, we also assumed that once the pressure reaches the threshold value of the terminal airways the subtended alveoli open immediately, that is, we did not assign a separate opening threshold pressure to the alveoli. Nevertheless, alveolar collapse can occur independently of airway closure.[9] Although Hughes and Rozenzweig[9] found that the pressure required to collapse airways and alveoli are quite similar, their respective opening threshold pressures could be quite different. The large atelectatic areas on the surface of degassed lungs clearly indicate massive alveolar collapse. In the present models the opening of atelectatic areas is absorbed in the threshold pressures of the last generation airways.

In model 1, another important assumption was that the opening threshold pressures are distributed uniformly. In model 2, we still have a uniform distribution between two limits, a and b. However, if the difference between b and a was small compared to unity, i.e., the full range of inflation pressure, the distribution of threshold pressures could be very sharp—more like a Gaussian. We found that the parameter a always approached 0 and b was close to 1. Thus, the data required that the distribution of the threshold pressures be wide and relatively uniform. As an additional verification, we replaced the uniform distribution in model 2 by an exponential distribution between 0 and 1. This model did not improve the fits to the $P-V$ data and also predicted an almost uniform distribution.

These findings apparently contradict the predictions of Gaver *et al.*[6] who measured the relationship between p_{th} and opening velocity u in thin-walled flexible tubes coated inside with liquids of different viscosity (μ) and surface tension (γ). They found that if the capillary number ($Ca=\mu u/\gamma$) is small, then $p_{th}\sim 8\gamma/R$, where R is the radius of the tube. This implies a deterministic relationship between p_{th} and R or the generation number such that smaller airways are increasingly more difficult to open. In a follow-up study, Naureckas *et al.*[13] using microfocal x-ray imaging, measured p_{th} as a function of airway diameter and found that their data could be well approximated by $p_{th}\sim 8\gamma/R$. Our primary assumption in model 2, on the other hand, was that the p_{th} does not have a generation number dependence. This, however,

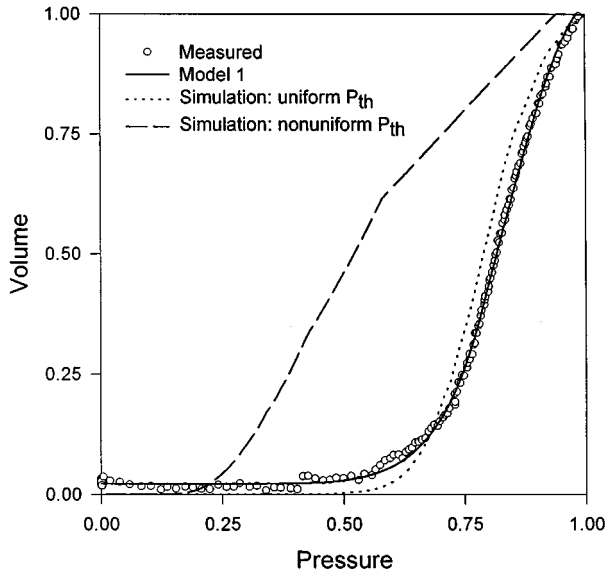

FIGURE 4. Normalized pressure–volume curves simulated directly using avalanches in a tree where, at the beginning of inflation, the first $N=10$ generations were assumed to be open and the last $n=10$ generations were assumed to be completely closed. The dotted line represents the cases where the opening threshold pressures were distributed uniformly between 0 and 1. The dashed line is a model where the threshold pressures were nonuniformly distributed increasing hyperbolically with the increasing generation number toward the periphery (see the text). The open symbols are the pressure–volume curve of lung No. 16 and the solid line is the fit of model 1.

may not contradict the $p_{th} \sim 1/R$ relationship as explained below.

The deterministic $p_{th} \sim 1/R$ relationship is different from the spatial distribution of threshold parameters. In the study by Naureckas *et al.*,[13] airways were selected without regard to their spatial location or generation number. Moreover, their data also demonstrate that for airways with practically the same diameter, the corresponding p_{th} can easily vary as much as 30%–50%. Thus, while p_{th} can inversely depend on airway diameter, its spatial distribution can still be wide and relatively uniform across the tree due to local variations in the physical quantities determining p_{th}. We recently argued[2] that there are several mechanisms that can balance the strong generational dependence suggested by Gaver *et al.*[6] These include geometry, local variations in R, γ, lining liquid thickness, airway wall thickness, airway wall elasticity, parenchymal tethering, and possibly smooth muscle tone.

There are no direct experimental data on the spatial distribution of p_{th}. We therefore examined this problem via simulating the $P-V$ curve during the first inflation in a model with $N=10$ and $n=10$, i.e., the first ten generations were open and the last ten generations were completely closed. We first distributed p_{th} uniformly, then calculated the $P-V$ curve for the given p_{th} distributions directly, based on simulating the avalanches in the tree. As shown in Fig. 4 (dotted line), when p_{th} is uniformly distributed, the simulated $P-V$ curve is in good accord with model 1 [Eq. (8)]. Note that the $P-V$ curve is smooth since in essence it is the average of the $P-V$ curves in 2^{10} subtrees each having ten generations. For comparison, in Fig. 4 we also plotted the $P-V$ curve of lung No. 16 together with the fit of model 1. The simulated and the measured $P-V$ curves are in good qualitative agreement. We also studied the case in which p_{th} had a strong generational dependence. When the mean of p_{th} is inversely proportional to the generation number, the volume increases with pressure again as a power law, but with an exponent that decreases as pressure increases (Fig. 4, dashed line). Thus, strong generational dependence of p_{th} results in a $P-V$ curve that is qualitatively very different from the one with a uniform p_{th} distribution and which is not consistent with any of the data. The main reason is that avalanches with a wide distribution of sizes do not occur in this model since as the generation number increases, threshold pressures tend to increase too and the likelihood that an avalanche proceeds through many generations is practically zero. Thus, while our modeling results do not strictly suggest that the distribution of threshold pressures is uniform in the periphery of the lung (i.e., the shape of the distribution could be quite different from a uniform one), the distribution itself is wide enough between 0 and 1 so that concerning the avalanche mechanism, the distribution is not essentially different from a uniform one.

Model Parameters

Model 1 has two free parameters, n, the order of completely closed subtrees and P_{low}. With regard to P_{low}, we note that it incorporates parallel subtrees into the model with their maximum threshold pressures P_{max} distributed between P_{low} and 1. This allows for certain parts of the lung to be fully open and driven by the local parenchymal elasticity while in other areas the opening process still contributes with discrete volume elements to the $P-V$ curve. This was necessary since the parameter P_{low} controls the location where the transition occurs from an almost constant volume to an almost constant pressure inflation. Additionally, if P_{low} was unity, the model would reduce to a single power law [Eq. (11)]. When $P_{low}<1$, the model 1 deviates from a single power law [Eq. (8)] as P approaches unity. As a consequence, as Fig. 4 demonstrates, the model is able to produce the inflection point also seen in the data and hence it does not need to include an explicit term for the alveolar surface film and tissue elasticity. Note that model 1 is now fit to the entire $P-V$ curve (in Fig. 3 both models

are fit only up to $P=0.85$). Model 2, on the other hand, is not able to follow the measured $P-V$ curve to high pressures. Thus, we tested the hypothesis that elasticity is not necessary. A multiplicative compliance term (normalized to 1) was included in Eq. (8) to account for the $P-V$ relation of the tissue which, however, did not significantly improve the fits and often reduced the uniqueness of the model parameters.

The parameter n is related to the size of the subtrees that was predicted to be closed at the beginning of inflation. The average value of n is 17, independent of the model. However, on an individual basis, this number cannot be interpreted as the exact number of closed generations in the lung, but rather as some average generation number. The size of the airways that are initially closed corresponding to generation 17 from the bottom is not obvious since, to our knowledge, there is no systematic evaluation of the airway tree in rabbits. If we assume that the last generation airways in our model correspond to terminal bronchioles, then the diameter of such an airway in a rat[28] or a dog[8] lung would be in the order of 1–2 mm at TLC. Studying the effects of parenchymal tethering on airway reopening Yap *et al.*[27] were able to produce airway closure by suction in airways having diameters of 2–3 mm which remained closed after eliminating the suction. Additionally, Hoppin *et al.*[7] noted that isolated lung lobes open quite unevenly. Some lobes open completely while others may remain entirely collapsed from which they concluded that even lobar bronchi can be intensely constricted. Overcoming such a threshold pressure would then lead to avalanches whose sizes can be a significant portion of a lobe. Furthermore, according to the rat airway model[28] the number of subtrees can be estimated to be between 40 and 100. This number is sufficiently large to justify the assumption that the maximum threshold pressures in the subtrees are distributed between P_{low} and 1 and that we calculate the average behavior of these subtrees.

Physiological Implications

Having discussed the most important features and assumptions of the model, we now address the different behavior of the $P-V$ curves seen in Figs. 2(A) and 2(B). The $P-V$ curve in Fig. 2(B) shows that following the rapid increase in V, the pressure temporarily decreases and then increases again. Our model is not consistent with this behavior. One reason could be that we assumed that the model is pressure driven whereas in the experiment volume was controlled. The rate of pressure increase has no effect on the model predictions since no dynamics is built into the model. On the other hand, in isolated rat lungs, Frazer and Weber[5] found that the pressure always showed a temporary decrease after the initiation of volume increase if the inflation flow rate was high. We do not find any correlation between this behavior and flow rate. However, our flow rates were very similar in the two groups of lungs corresponding to the two types of $P-V$ curves shown in Fig. 2. We were not specifically setting out to study this phenomenon and hence the range of flow rates may not have been sufficiently wide to find a correlation. On the other hand, there was a negative correlation between flow rate and P_{low} which implies that by increasing flow rate, P_{low}, i.e., the pressure threshold at which a massive airway opening is initiated, has a tendency to decrease. This has two implications. First, we note that Gaver *et al.*[6] found that p_{th} increases linearly with the velocity of the air finger opening a collapsed flexible tube. This is not supported by our results and hence the primary mechanism for closure may be compliant collapse and not liquid bridging in degassed lungs, a conclusion recently also reached by Otis *et al.*[15] Second, one may speculate that the decrease in pressure in the transition zone [Fig. 2(B)] could be due to the dynamics of airway reopening. So far we have assumed that avalanches are an abrupt and instantaneous process. However, opening of an airway requires some time and hence the progression of avalanches may not occur instantaneously. When P_{tp} in the lung exceeds the p_{th} of a branch, that airway opens and consequently the local air volume is redistributed into a larger volume and the overall pressure or P_{tp} is reduced. The redistribution of air in the newly opened volume could be faster than the time required to open the next airway (which could otherwise be opened by the value of P_{tp}). This is similar to a situation where the threshold pressures are dynamically changed by the avalanches and then parenchymal instabilities may develop as described by Stamenović.[23] Thus, taking into account the dynamics of gas redistribution may lead to a $P-V$ relationship with a negative compliance. Nevertheless, while the exact mechanism for this instability is not clear, the avalanche mechanism still governs the transition from an almost constant volume inflation to the rapid filling of the lung at an almost constant pressure.

In an attempt to verify the model and to provide some physiological implications of the results, we applied both models to a condition which was not used to develop these models. We fit the $P-V$ curve of one lung which was lavaged with 3-dimethyl siloxane, a liquid of constant surface tension of 16 dyn/cm.[20] While model 1 is not able to fit the data, model 2 provided an excellent fit as shown in Fig. 5. Interestingly, the order of the tree was 2 and 1.2 in models 1 and 2, respectively. The range over which the threshold pressures were distributed in model 2 was very narrow, between 0.2 and 0.5. Thus, since model 1 includes a uniform distribution between 0 and 1, these results imply that the distribution of threshold pressures is rather narrow. Both models predict that the avalanche behavior does not dominate the $P-V$

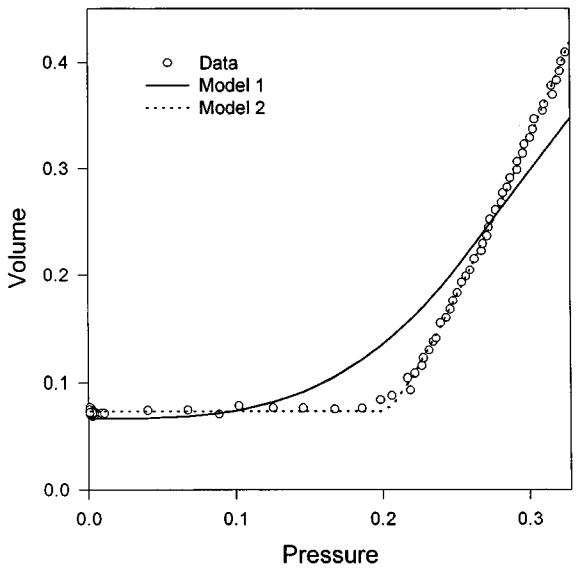

FIGURE 5. Normalized *P–V* curve of the inflation limb (symbols) in a lung lavaged with 3-dimethyl siloxane, a liquid of constant surface tension of 16 dyn/cm (Ref. 20) and the fits of model 1 (solid line) and model 2 (dashed line).

curve as the maximum size of an avalanche would be 1 or 2. Additionally, the $P-V$ curve is such that until a transition pressure is reached ($P=0.2$) there is no volume change which is then followed by essentially a linear $P-V$ curve (n is almost 1). If the threshold pressures are determined by the $p_{th} \sim \gamma/R$ relationship,[6] then, since γ is constant not dependent on lung volume, the smallest threshold pressure would then be directly proportional to γ of the lavage liquid. This is in good agreement with the findings of Smith and Stamenović[20] that the transition pressure is linearly related to the surface tension. Their data also demonstrated that the slope of the linear increase of the $P-V$ curve did not depend very much on the surface tension. In model 2, this slope is determined by the width of the threshold distribution. Since this width is small (0.3) compared to unity (i.e., when the lung has natural surfactant), regions in the lung periphery successively open, but not via avalanches. This picture is consistent with the fact that lungs lavaged with a liquid of high and constant surface tension do not trap air since at low lung volumes, the high surface tension does not allow the larger airways to close up before small airways close.

In summary, we described the first inflation of degassed, excised lungs with a relatively simple model that provides information on the distribution of opening threshold pressures and the range of airway closure in the collapsed lung. Besides the fact that all mammals undergo at least once such a $P-V$ curve when they are born,[18] these conditions can also occur following an injury or surgery such as cardiopulmonary bypass. The implications are that in order to open all airway pathways in a collapsed lung, the complete transition from the state of increasing pressure at constant volume through increasing volume at almost constant pressure to a state where both increase must be achieved. Similar closing and reopening phenomena occur in other organs such as the heart. The importance of these phenomena was emphasized by Sherman *et al.*:[19] ''the high value of critical opening pressure may be responsible for myocardial injury associated with ischemic cardiac arrest during open-heart surgery.'' Therefore, the mechanism of filling the lungs via the statistical process of airway reopening described here may find more general applications than only the $P-V$ curve of the lungs.

ACKNOWLEDGMENTS

The authors thank NSF (BES 9503008 and INT 9604250), CNPq and NIH (HL-33009) for support, and Dr. H. Kitaoka for many helpful discussions.

REFERENCES

[1] Bachofen, H., J. Hildebrandt, and M. Bachofen. Pressure–volume curves of air- and liquid-filled excised lungs–surface tension *in situ*. *J. Appl. Physiol.* 29:422–431, 1970.

[2] Barabási, A-L., S. Buldyrev, H. E. Stanley, and B. Suki. Avalanches in the lung: A statistical mechanical model. *Phys. Rev. Lett.* 76:2192–2195, 1996.

[3] Cheng, W., D. S. DeLong, G. N. Franz, E. L. Petsonk, and D. G. Frazer. Contribution of opening and closing of lung units to lung hysteresis. *Respir. Physiol.* 102:205–215, 1995.

[4] Csendes, T. Nonlinear parameter estimation by global optimization—efficiency and reliability. *Acta Cybern.* 8:361–370, 1988.

[5] Frazer, D. G., and K. C. Weber. Trapped air in ventilated excised rat lungs. *J. Appl. Physiol.* 40:915–922, 1976.

[6] Gaver III, D. P., R. W. Samsel, and J. Solway. Effects of surface tension and viscosity on airway reopening. *J. Appl. Physiol.* 69:74–85, 1992.

[7] Hoppin, Jr., F. G., J. C. Stothert, Jr., I. A. Greaves, Y-L. Lai, and J. Hildebrandt. Lung recoil: Elastic and rheological properties. In: Handbook of Physiology, The Respiratory System, Mechanics of Breathing. Bethesda, MD: Am. Physiol. Soc., 1986, Sec. 3, Vol. III, Chap. 13, pp. 195–215.

[8] Horsfield, K., W. Kemp, and S. Phillips. An asymmetrical model of the airways of the dog lung. *J. Appl. Physiol.* 52:21–26, 1982.

[9] Hughes, J. M. B., and D. Y. Rosenzweig. Factors affecting trapped gas volume in perfused dog lungs. *J. Appl. Physiol.* 29:332–339, 1970.

[10] Hughes, J. M. B., D. Y. Rosenzweig, and P. B. Kivitz. Site of airway closure in excised dog lungs: Histologic demonstration. *J. Appl. Physiol.* 29:340–344, 1970.

[11] Macklem, P. T., D. F. Proctor, and J. C. Hogg. The stability of peripheral airways. *Respir. Physiol.* 8:191–203, 1970.

[12] Mead, J., J. L. Whittenberg, and E. P. Radford, Jr. Surface tension as a factor in pulmonary volume–pressure hystersis. *J. Appl. Physiol.* 9:191–196, 1957.

[13] Naureckas, E. T., C. A. Dawson, B. S. Gerber, D. P. Gaver III, H. L. Gerber, J. H. Linehan, J. Solway, and R. W. Samsel. Airway reopening pressure in isolated rat lungs. *J. Appl. Physiol.* 76:1372–1377, 1994.
[14] Otis, D. R. An investigation of the mechanisms responsible for pulmonary airway closure. Ph.D. Thesis. MIT: Cambridge, MA, 1995.
[15] Otis, D. R., Jr., F. Petak, Z. Hantos, J. J. Fredberg, and R. D. Kamm. Airway closure and reopening assessed by the alveolar capsule oscillation technique. *J. Appl. Physiol.* 80:2077–2084, 1996.
[16] Peták, F., Z. Hantos, A. Adamicza, D. R. Otis, and B. Daróczy. Volume dependence of terminal airway impedance in isolated dog lungs (Abstract). *Eur. Respir. J.* 6:403S, 1993.
[17] Radford, Jr., E. P. Recent studies of the mechanical properties of mammalian lungs. In: Tissue Elasticity, edited by J. W. Remington. Washington DC: Am. Physiol. Soc., 1957, pp. 177–190.
[18] Scarpelli, E. M. Surfactant and the Lining of the Lung. Baltimore, MD: The Johns Hopkins University Press, 1988.
[19] Sherman, I. A., J. Grayson, and C. E. Bayliss. Critical closing and critical opening phenomena in the coronary vasculature of the dog. *Am. J. Physiol.* 238 (*Heart Circ. Physiol.)* 7:H533–H538, 1980.
[20] Smith, J. C., and D. Stamenović. Surface forces in lungs. I. Alveolar surface tension-lung volume relationship. *J. Appl. Physiol.* 60:1341–1350, 1986.
[21] Smith, J. C., and W. Mitzner. Analysis of pulmonary vascular interdependence in excised dog lobes. *J. Appl. Physiol.* 48:450–467, 1980.
[22] Stamenović, D., and J. C. Smith. Surface forces in lungs. II. Microstructural mechanics and lung stability. *J. Appl. Physiol.* 60:1351–1357, 1986.
[23] Stamenović, D. The mixture of phases and elastic stability of lungs with constant surface forces. *Math. Model.* 7:1071–1082, 1986.
[24] Sujeer, M. K., S. V. Buldyrev, S. Zapperi, J. S. Andrade, Jr., H. E. Stanley, and B. Suki. Volume distributions of avalanches in lung inflation: A statistical mechanical approach. *Phys. Rev. E* 56:3385–3394, 1997.
[25] Suki, B., A-L. Barabási, Z. Hantos, F. Peták, H. E. Stanley, and B. Suki. Avalanches and power law behavior in lung inflation. *Nature (London)* 368:615–618, 1994.
[26] Tepper, R. S., S. J. Gunst, C. M. Doerschuk, X. Shen, and W. Bray. Effect of transpulmonary pressure on airway closure in immature and mature rabbits. *J. Appl. Physiol.* 78:505–512, 1995.
[27] Yap, D. Y. K., W. D. Liebkemann, J. Solway, and D. P. Gaver III. Influences of parenchymal tethering on the reopening of closed pulmonary airways. *J. Appl. Physiol.* 76:2095–2105, 1994.
[28] Yeh, H. C., G. M. Schum, and M. J. Duggan. Anatomic models of the tracheobronchial and pulmonary regions of the rat. *Anat. Rec.* 195:483–492, 1979.
[29] Zapperi, S., K. B. Lauritsen, and H. E. Stanley. Self-organized branching processes: Mean-field theory for avalanches. *Phys. Rev. Lett.* 75:4071–4074, 1995.